Acc. Chem. Res. **2000,** *33,* 269−277

Molecular Photovoltaics

ANDERS HAGFELDT† AND
MICHAEL GRÄTZEL*,‡

Department of Physical Chemistry, Angström Solar Center, University of Uppsala, S75121 Uppsala, Sweden, and Insitute of Photonics and Interfaces, Swiss Federal Institute of Technology, CH-1015 Lausanne, Switzerland

Received June 24, 1999

ABSTRACT

The dye-sensitized nanocrystalline injection solar cell employs transition metal complexes for spectral sensitization of mesoporous TiO_2 films together with suitable redox electrolytes or amorphous organic hole conductors. Light harvesting occurs efficiently over the whole visible and near-IR range due to the very large internal surface area of the films. Judicious molecular engineering allows the photoinduced charge separation to occur quantitatively within a few femtoseconds. The certified overall power conversion efficiency of the new solar cell for AM 1.5 solar radiation stands presently at 10.4%.

Scientists have been infatuated with photoelectric molecules ever since the discovery of photography more than 100 years ago. The first panchromatic film, able to render the image of a scene realistically into black and white, followed on the work of Vogel in Berlin after 1873,[1] in which he associated dyes with silver halide grains. The first sensitization of a photoelectrode was reported shortly thereafter, using a similar chemistry.[2] However, the clear recognition of the parallelism between the two procedures, the realization that the same dyes can function in both,[3] and the verification that the operating mechanism is by injection of electrons from photoexcited dye molecules into the conduction band of the semiconductor substrates[4] date to the 1960s. In subsequent years the idea developed that the dye could function most efficiently if chemisorbed on the surface of a semiconductor.[5,6] The concept emerged to use dispersed particles to provide a sufficient interface,[7] and then particulate photoelectrodes were employed.[8] Titanium dioxide became the semiconductor of choice.[9] The material has many advantages: it is cheap, abondant, nontoxic, and biocompatible, and is widely used in health care products as well as in paints. The standard dye at the time was tris(2,2′-bipyridyl, 4,4′-carboxylate)ruthenium(II), the function of the carboxylate being the attachment by chemisorption of the chromophore onto the oxide substrate.[8,9] In 1991,[10] the first dye-sensitized nanocrystalline solar cell with a conversion yield of 7.1% was announced, and presently the certified efficiency is over 10%.

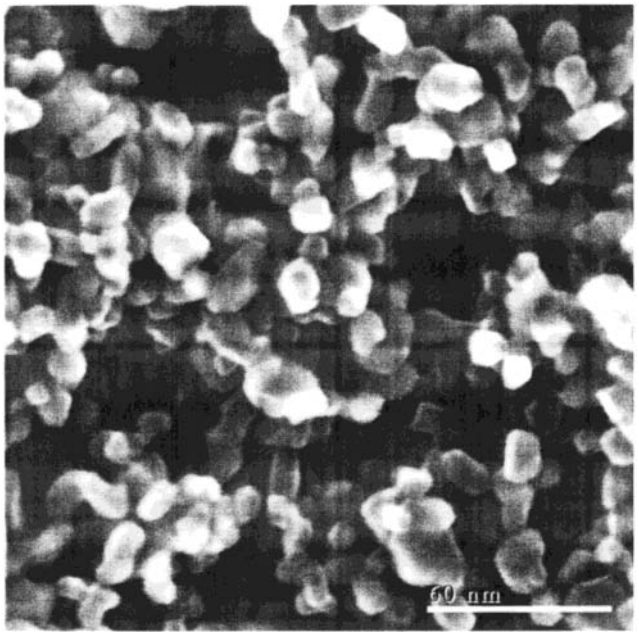

FIGURE 1. Scanning electron microscope pattern of a typical nanocrystalline TiO_2 film.

At the heart of the device is the mesoporous oxide layer composed of a network of TiO_2 nanoparticles which have been sintered together to establish electronic conduction (Figure 1). The prevailing morphologies of the anatase nanoparticles are square bipyramidal, pseudocubic, and stablike. According to transmission electron microscopy measurements,[11] the (101) face is the most exposed, followed by (100) and (001) orientations. Attached to the surface of the nanocrystalline film is a monolayer of the charge-transfer dye. Photoexcitation of the latter results in the injection of an electron into the conduction band of the oxide (Figure 2). The original state of the dye is subsequently restored by electron donation from the electrolyte, usually an organic solvent containing the iodide/triioide redox system. The regeneration of the sensitizer by iodide intercepts the recapture of the conduction band electron by the oxidized dye. The iodide is regenerated, in turn, by reduction of triiodide at the counter electrode, the circuit being completed through the external load. The voltage generated under illumination corresponds to the difference between the Fermi level of the electron in the solid and the redox potential of the electrolyte. Overall, electric power is generated without permanent chemical transformation.

A solid-state version of the cell is the sensitized heterojunction (Figure 3). Here, the electrolyte is replaced

Anders Hagfeldt was born in Norrkoping, Sweden, in 1964. He received a Ph.D. (1993) in physical chemistry from the University of Uppsala and worked as a postdoctoral fellow with Professor Michael Grätzel at EPFL in Lausanne, Switzerland. At present he is an Associate Professor at the Department of Physical Chemistry, Uppsala University, and Program Secretary of Angstrom Solar Center. He is also a fellow of LEAD (Leadership for Environment and Development).

Michael Grätzel is a professor at the Swiss Federal Institute of Technology in Lausanne, Switzerland, where he directs the Institute of Photonics and Interfaces. His laboratory initiated studies in the domain of nanocrystalline semiconductors and mesoporous oxide semiconductor films and developed the dye-sensitized nanocrystalline solar cell. Prof. Grätzel, who is the author of over 400 publications, has received a number of awards and honorary lectureships including an honorary doctors degree from the University of Uppsala, Sweden. He is a member of several editorial boards.

† University of Uppsala.
‡ Swiss Federal Institute of Technology.

10.1021/ar980112j CCC: $19.00
Published on Web 02/23/2000

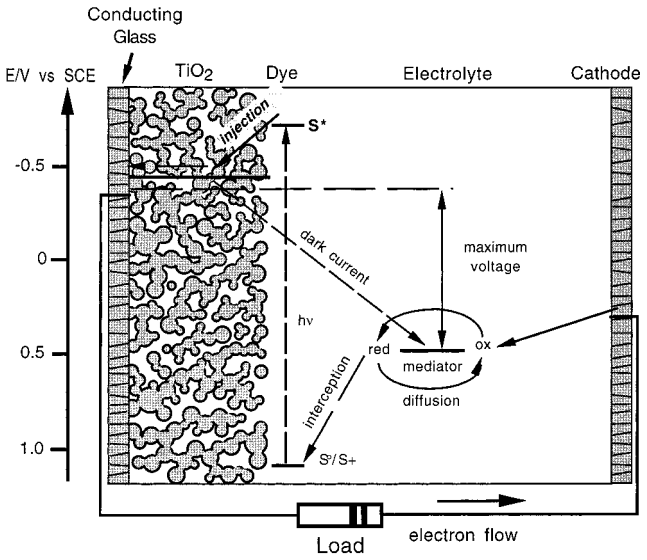

FIGURE 2. Schematic representation of the principle of the nanocrystalline injection cell to indicate the energy level in the different phases. The cell voltage observed under illumination corresponds to the difference in the quasi-Fermi level of the TiO_2 under illumination and the electrochemical potential of the electrolyte. The latter is equal to the Nernst potential of the iodide/triiodide redox couple used to mediate charge transfer between the electrodes.

by a wide band gap inorganic semiconductor of p-type polarity, such as CuI[12] or CuSCN,[13] or a hole-transmitting solid, e.g., an amorphous organic arylamine.[14] The excited dye injects electrons in the n-type oxide, and it is regenerated by hole injection in the p-type marterial.

This Account focuses on the molecular engineering of efficient heterogeneous electron-transfer sensitizers and scrutinizes the factors that afford quantitative charge separation at the dye−semiconductor interface. The mechanism of electron percolation across the nanocrystalline oxide film is also dicussed. Finally, perspectives for future development are presented.

Molecular Engineering of Heterogeneous Charge-Transfer Sensitizers

The ideal sensitizer for a single-junction photovoltaic cell should absorb all light below a threshold wavelength of about 900 nm. In addition, it should be firmly grafted to the semiconductor oxide surface and inject electrons to the conduction band with a quantum yield of unity. Its redox potential should be sufficiently high that it can be regenerated rapidly via electron donation from the eletrolyte or a hole conductor. Finally, it should be stable enough to sustain at least 10^8 redox turnovers under illumination corresponding to about 20 years of exposure to natural light. The best photovoltaic performance in terms of both conversion yield and long-term stability has so far been achieved with polypyridyl complexes of ruthenium and osmium.[15−18] Sensitizers having the general structure $ML_2(X)_2$, where L stands for 2,2′-bipyidyl-4,4′-dicarboxylic acid, M for Ru or Os, and X for halide, cyanide, thiocyanate, or water,[15,17] are particularly promising. In recent years, the ruthenium complex *cis*-$RuL_2(NCS)_2$, known as the N3 dye, has emerged as the paradigm of a heterogeneous charge-transfer sensitizer for mesoporous solar cells. Discovered in 1993,[15] its performance has been unmatched by hundreds of other complexes that have been synthesized and tested since then. Only recently, a credible challenger has been found with the black dye tri(cyanato)-2,2′,2″-terpyridyl-4,4′,4″-tricarboxylate)ruthenium(II) that exhibits better near-IR photoresponse than N3.[18]

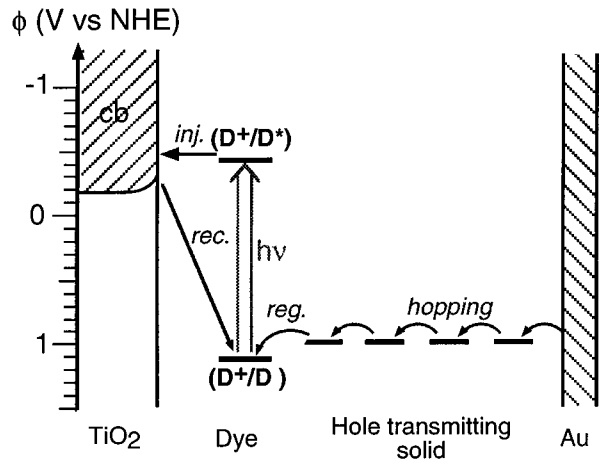

FIGURE 3. Dye-sensitized heterojunction solar cell where the electrolyte in Figure 1 is replaced by an organic hole conductor. Energy levels of the different redox species and TiO_2 vs NHE are shown. Electron-transfer reactions are symbolized by black arrows.

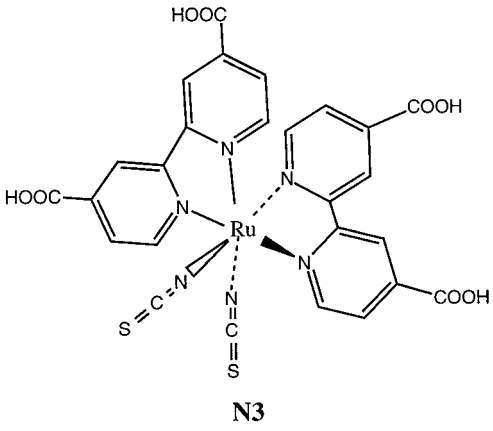

N3

Configuration of Surface-Anchored N3 Sensitizer. The crystal structure of N3 is shown in Figure 4. Ruthenium adopts a distorted octahedral geometry in the complex, one of the carboxylate groups, viz. C(17)O(1)O(2), being skewed up to 30° from the ideal orientation which is coplanar to the bipyridyl moiety. The thiocyanate groups are bound through the nitrogen, although the S-bonded isomer does appear as an intermediate species and as a final impurity during N3 synthesis.[19] Surface derivatization of the mesoporous oxide film is normally performed by dipping it into a solution of N3 in a 50/50 (v/v) solvent mixture of acetonitrile/*tert*-butanol. A monolayer of sensitizer is formed spontaneously through attachment via the carboxylic acid anchoring groups. The adsorption follows a Langmuir isotherm. The binding constant is

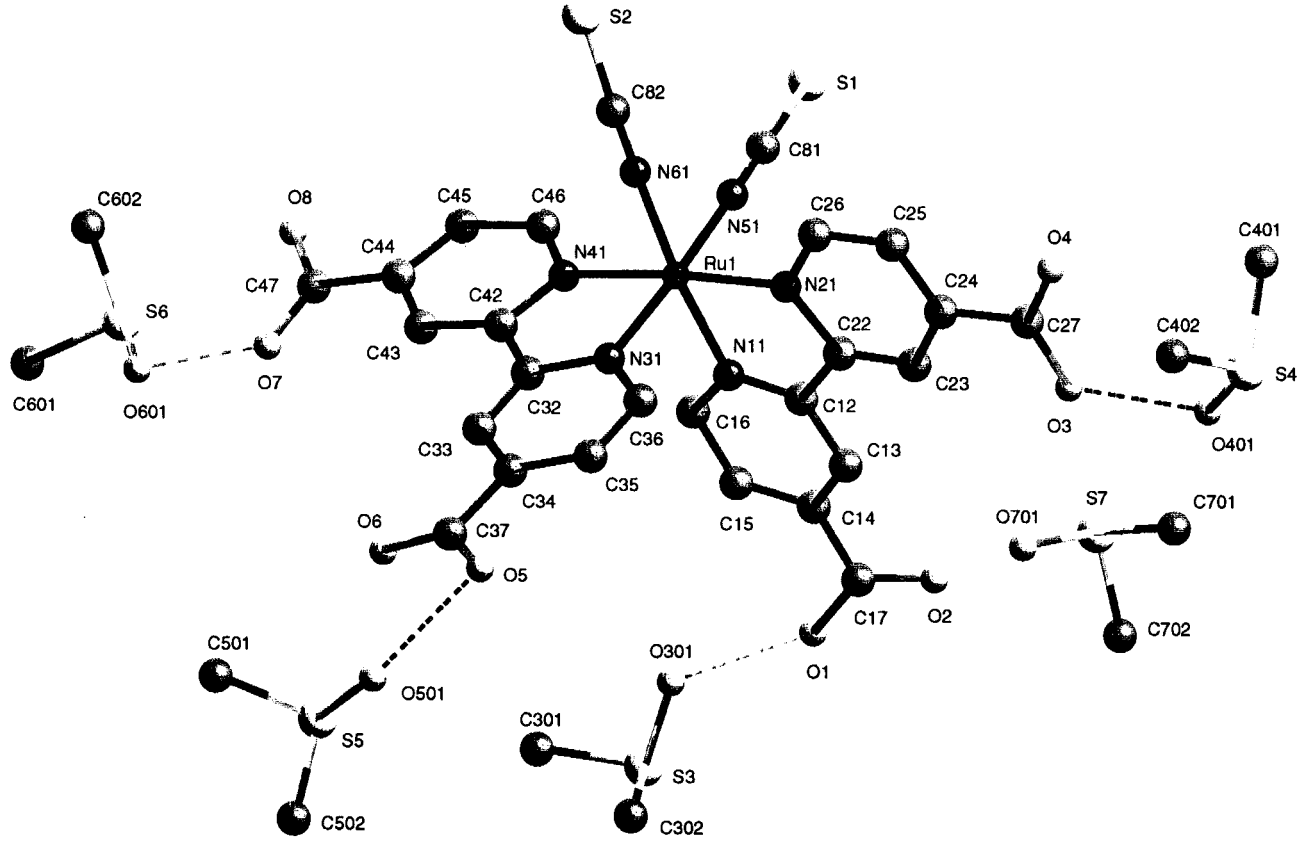

FIGURE 4. X-ray crystal structure of N3.

5×10^4 M^{-1}, and the area occupied by one N3 molecule at the anatase surface at full monolayer coverage is 1.65 nm^2.

The interaction between the carboxylic group and the TiO_2 is of fundamental importance in determining the geometrical structure of the adsorbed dye state and influencing the electronic coupling with the Ti(3d) conduction band orbital manifold. Molecular dynamics calculations have been used to model the interaction of this sensitizer with the (101) surface plane of anatase.[20] The most likely configuration supported by recent IR analysis[21] is shown in Figure 5. The dye is attached via two of its four carboxylate groups. The carboxylate either bridges two adjacent rows of titanium ions through bidentate coordination or interacts with surface hydroxyl groups through hydrogen bonds. Of the two remaining carboxylate groups, one is ionized while the other remains in the protonated state.

Model studies, using the L ligand of N3 adsorbed onto single-crystal TiO_2 (110) rutile, investigated by means of X-ray photoelectron spectroscopy, X-ray absorption spectroscopy, and quantum chemical calculations,[22] are also in favor of the bridging bidentate configuration. The ligand is oriented at an angle of about 40° with respect to the (001) crystallographic direction. Interestingly, from the calculations it was found that, in addition to the bidentate carboxylate−titanium linkage described above, the monodentate ester bond is also thermodynamically stable. However, the former bonding is stronger and thus would be the preferred binding configuration for the N3 dye.

Energy Levels and Orbital Configuration. The interfacial electron-transfer events will be strongly affected by the electronic structure of the dye in the adsorbed state and the energy level matching between its excited state and the conduction band of the semiconductor. Generally, the optical transition of Ru complexes has metal-to-ligand charge-transfer (MLCT) character. Excitation of the dye involves transfer of an electron from the metal to the π^* orbital of the ligand. N3 has two such transitions in the visible region. The absorption maxima in ethanolic solution are located at 518 and 380 nm, the extinction coefficients being 1.33×10^4 and 1.3×10^4 M^{-1} cm^{-1}, respectively. The complex emits at 750 nm, the excited-state lifetime being 60 ns.[15]

Results from an ab initio calculation of a decarboxylated N3 complex are presented in Figure 6, showing the highest occupied (HOMO) and lowest unoccupied (LUMO) molecular orbital surfaces.[23] We note that the HOMO level is actually shared by both the Ru metal and the NCS ligands. Photoelectron spectroscopy has been used to study the density of states of the N3 valence levels by photon energy and angular-dependent spectra.[24] These experiments confirm that both Ru4d and atomic orbitals centered on the −NCS groups, in particular S3p wave functions, contribute to the frontier orbitals of the complex. In a photovoltaic cell, the oxidized dye, after electron injection to the conduction band of the oxide, should quickly be reduced by a redox species in the surrounding electrolyte. The observation that the outermost orbital contains a substantial amount of S3p-character from the

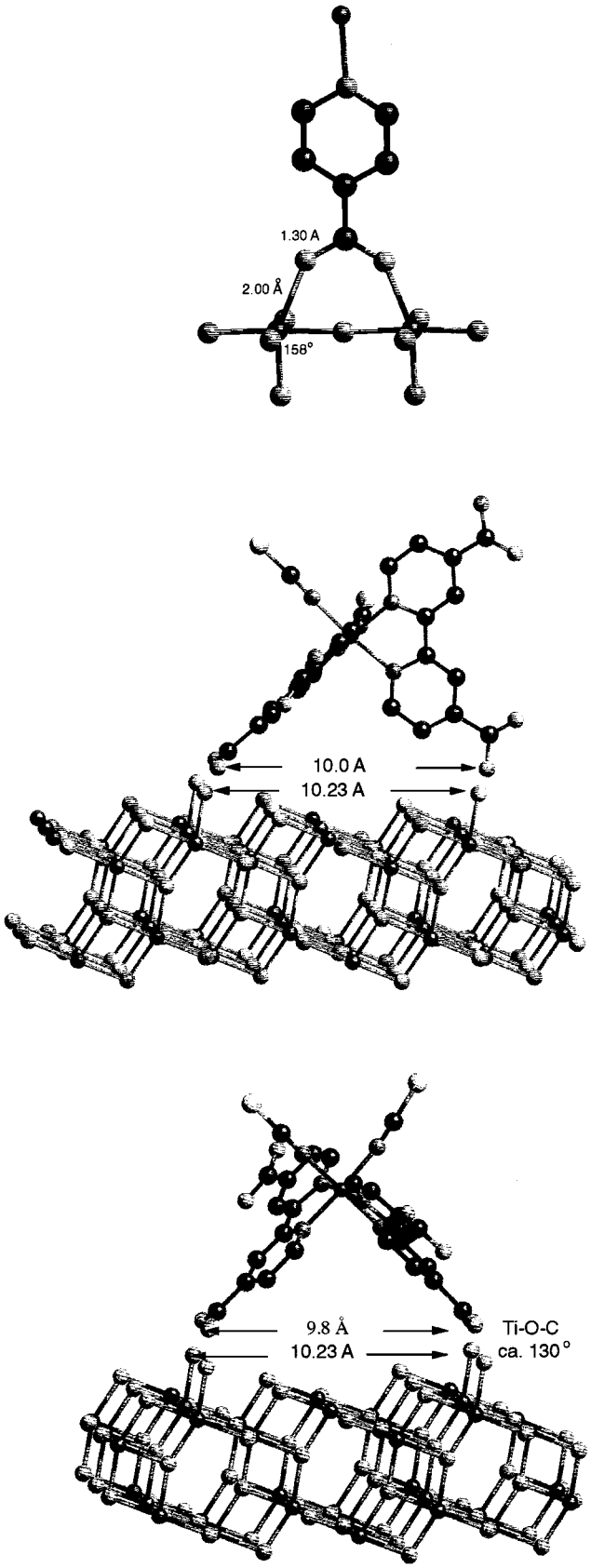

FIGURE 5. Anchoring of the N3 dye on the (101) surface of anatase.

−NCS groups may play an important role in this process. The −NCS groups point in the direction of the electrolyte, which may facilitate reduction by I^-, making it particularly suitable for highly efficient solar cells. The LUMO in Figure 6 is concentrated on the π^* structure of the ligands. Thus, the absorption bands of $Ru(bpy)_2(NCS)_2$ can be assigned to a RuNCS−bpy(π^*) transition. Preliminary calculations of the carboxylated N3 indicate that the bpy rings share their LUMO with the COOH groups, enhancing electronic coupling to the TiO_2 conduction band states.

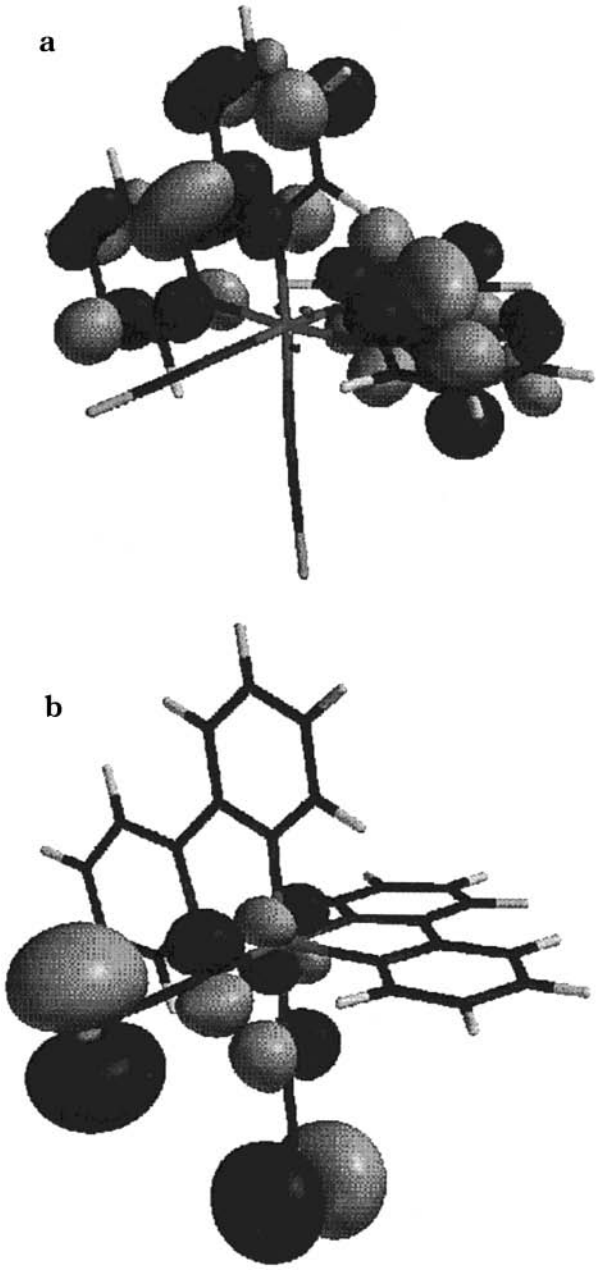

FIGURE 6. (a) Calculated HOMO and (b) LUMO molecular orbital surfaces for $Ru(bpy)_2(NCS)_2$.

The energetics at the dye/metal oxide was summarized in our previous review article,[25] in which data were taken from different optical and electrochemical measurements. Recently, the valence level spectra from unsensitized as well as sensitized nanostructured TiO_2 electrodes have been directly derived from photoelectron spectroscopic methods.[22] Figure 7 shows the density of states in the valence region for an N3-derivatized nanostructured TiO_2 film together with an energy level diagram. The HOMO orbital of the complex can clearly be distinguished above

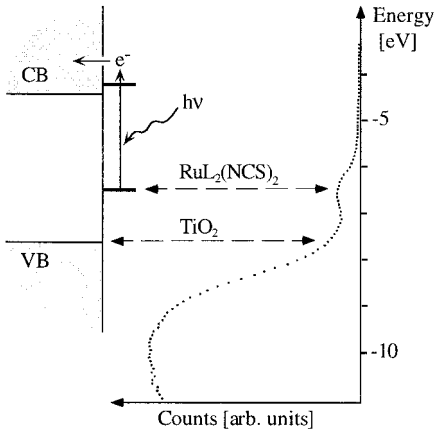

FIGURE 7. Valence band spectrum of a nanostructured TiO_2 film sensitized with N3.

the valence band edge of the semiconductor. Its position fits well with the energy requirements for efficient electron injection. The level of the vibronic state produced by 530-nm excitation of the dye is about 0.25 eV above the conduction band edge. For the 0−0 transition of N3 (ΔE = 1.65 eV[15]), the excited-state level matches the lower edge of the conduction band. This energy was estimated by using a difference in the valence band edge position and HOMO level position taken at the maximum of the density of states of 1.2 eV (with an uncertainty of about 0.1 eV), an absorption maximum for the dye of 2.3 eV, and a band gap for anatase TiO_2 of 3.2 eV. This possibility of determining the position of the outermost dye level in the semiconductor band gap is of particular interest in comparing different types of dyes in the search for chromophores having optimized energy level matching between the dye and the oxide and the dye and the redox couple.

Femtosecond Electron Injection. One of the most astounding findings over the past few years concerns the rate of electron injection from the excited N3 dye in the TiO_2 conduction band. Although assignments of transient spectra are still under debate,[26−29] it is now generally accepted that this interfacial redox reaction is one of the fastest chemical processes known to date occurring in the femtosecond time regime. In a recent elegant experiment,[30] mid-IR spectroscopy was used to probe directly the buildup of electron concentration inside the semiconductor. Careful examination at different wavelengths and time scales yielded a double exponential with rise times of 50 ± 25 fs (>84%) and 1.7 ± 0.5 ps (<16%). The slower component was very sensitive to the sample condition, and the exact origin is still unknown. A challenge for future research on these molecular photovoltaic systems is to explain the reasons for the ultrafast injection. It appears also that the anchoring carboxylic groups do not have to be conjugated to the π electron system of the chromophore for efficient electron transfer[31] to take place. There is a need for detailed theoretical modeling of the kinetics. Further experimental studies will focus on the participation of hot vibronic states in the electron injection which manifests itself by wavelength-dependent quantum yields.[32,33]

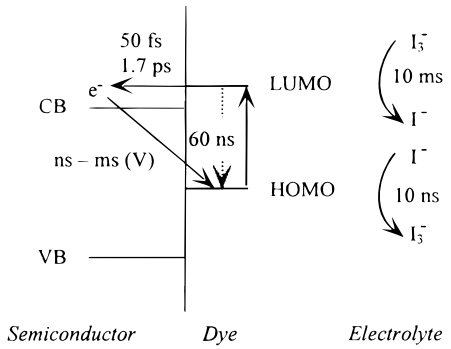

FIGURE 8. Schematic of the kinetics at the TiO_2/N3/electrolyte interface.

The Recapture of the Injected Electron and Its Interception. The kinetics of back-electron-transfer kinetics from the conduction band to the oxidized sensitizer follow a multiexponential time law, occurring on a microsecond to millisecond time scale. The reasons suggested for the relatively slow rate of the back-reaction transfer reaction are (i) weak electronic coupling between the electron in the solid and the Ru(III) center of the oxidized N3, (ii) trapping of the injected electron, and (iii) the kinetic impediment due to the inverted Marcus region.[34] Durrant and co-workers have presented some new data on this issue, showing the reaction to be strongly dependent on applied potential.[35] This may be of relevance for the performance of the cell and should be considered in the modeling of the electrical performance together with the reaction between I_3^- and conduction band electrons.[36] The latter process has been found to be second order with respect to the I_3^- concentration with a time constant of about 10 ms at 1 sun.[37]

The interception of the oxidized dye by the electron donor in the electrolyte, i.e., iodide, is crucial for obtaining good collection yields and high cycle life of the sensitizer. For N3, time-resolved laser experiments have shown the interception to take place within about 10 ns under the conditions applied in the solar cell. The $N3/N3^+$ couple shows reversible behavior in different organic solvents, the standard redox potential in acetonitrile being $E^\circ = 0.83$ V vs SCE.[38] The lower limit of 1 s can be derived for the lifetime of the oxidized dye from cyclic voltammetry. This means that the interception is 10^8 times faster than the intrinsic lifetime of the oxidized sensitizer, explaining the fact that N3 can sustain 100 million turnovers in continuous solar cell operation without loss of performance. Lack of adequate conditions for rapid regeneration of the dye leads to dye degradation. A summary of the possible electron-transfer pathways at the dye/semiconductor interface together with observed kinetic data is shown in Figure 8.

Electron Percolation through the Mesoporous Oxide Film

When the dye-sensitized mesoporous solar cell was first presented, perhaps the most puzzling phenomenon was the highly efficient charge transport through the nanocrystalline TiO_2 layer. The mesoporous electrodes are very

much different compared to their compact analogues because (i) the inherent conductivity of the film is very low, (ii) the small size of the individual colloidal particles does not support a built-in electrical field, and (iii) the oxide particles and the electrolyte-containing pores form interpenetrating networks whose phase boundaries produce a junction of huge contact area. These films may be viewed as an ensemble of individual particles through which electrons can percolate by hopping from one crystallite to the next, rather than regarding them as perforated compact electrodes,[25] suggesting a bottom-up approach to rationalizing the transport phenomena.

Charge transport in mesoporous systems is under keen debate today,[39−43] and only the most important questions can be addressed here. How are the electrons moving? Is their flow through the nanoparticle film to the collector electrode merely diffuse or is it driven by an electric field? Is the electric current space charge controlled? A first attempt to model carrier transport in nanocrystalline TiO_2 films suggested diffusion to be the operative mechanism.[39] However, it turned out to be erroneous to describe the electron motion by a fixed value for the diffusion coefficient. The transport is complex as it involves trapping and detrapping of electrons. The traps have different depths, leading to a distribution of trapping and detrapping times. Which type of trap the electron visits during its random walk through the oxide film depends on its quasi-Fermi level under illumination, i.e., on the light intensity.[40] At low light levels, deep traps participate in the electron motion, and a slow transport, with a correspondingly low diffusion coefficient $D(e^-)$ is expected. Increasing the light intensity means that deeper trap states are filled under steady-state conditions. The transport will be faster since it involves only shallow traps, resulting in a higher value for $D(e^-)$. The central importance of trap states in these systems has recently been discussed by Nelson,[43] who applied a dispersive transport model based on the continuous-time random-walk theory of Scher and Montroll.[44]

Another currently debated issue concerns space charge control of the photocurrent. It is generally assumed that the negative charge of the moving electron is efficiently screened by cations in the electrical double layer surrounding the semiconductor nanoparticles, making it move with its image charge as an essentially neutral species. However, there is evidence that the charge compensation on the electrolyte side of the junction can lag behind the electron movement, notably in ion-paired organic electrolytes when high photocurrents are drawn. Thus, in photocurrent transient measurements it was observed that the photocurrent response times became longer with decreasing electrolyte concentration.[45] Also, the calculated value of the effective diffusion coefficient, 1.5×10^{-5} cm^2/s, is several orders of magnitude smaller than that in the bulk crystalline material and strikingly similar to the diffusion constant of ions in the solution. The dynamics and molecular description of the screening process are issues of great interest for future studies. We note that mass transport in the electrolyte in mesoporous

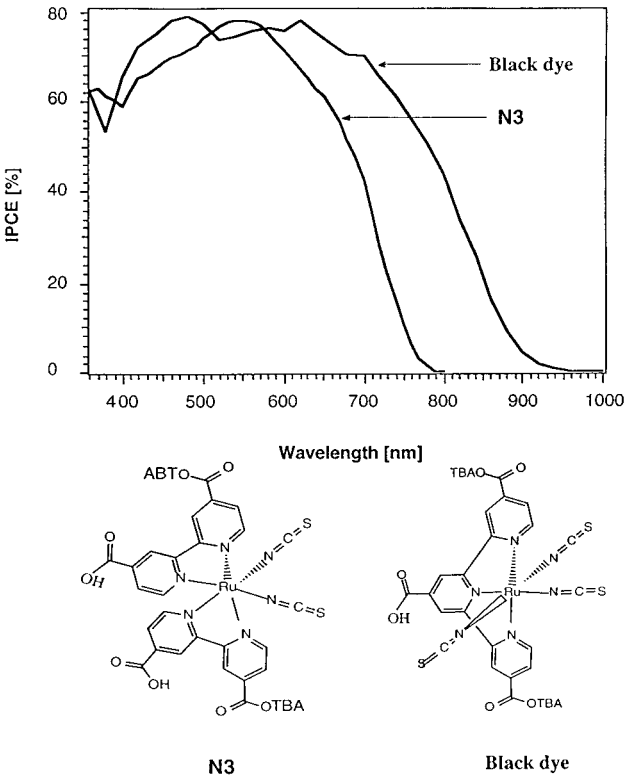

FIGURE 9. Spectral response curve of the photocurrent for the DYSC sensitized by N3 and the black dye. The incident photon to current conversion efficiency is plotted as a function of wavelength.

systems has been modeled[46] and a description of a coupled electronic-ionic motion presented,[36] albeit by employing a constant value for the electron diffusion coefficient.

Thus, although a lot of data and ideas concerning the charge transport process in mesoporous films have been presented, the picture is far from being complete. Where are the electrons (surface or bulk)? How many electrons are there per particle? Schlichthörl et al.[37] have calculated the steady-state carrier concentration in full sunlight to correspond to about one electron per TiO_2 particle. However, using this value together with a diffusion coefficient of 1.5×10^{-5} cm^2/s, one obtains a resistance for the illuminated nanocrystalline film which is at least 1000 times higher than the experimentally observed value. This discrepancy may be explained by the recent suggestion that the photodoping of the anatase particles results in a Mott transition, strongly increasing their conductivity.[47] Clearly, the central question which remains to be answered is how, in the dye-sensitized liquid-junction solar cell, an initially very poorly conducting network of anatase nanoparticles can attain the excellent photocurrent−voltage characteristics, i.e., fill factor of 0.7 at a current density of 20.5 mA/cm^2, presented below.

Photovoltaic Performance

Figure 9 compares the spectral response of the photocurrent observed with the N3 and the black dye sensitizer. The incident photon to current conversion efficiency (IPCE) of the solar cell is plotted as a function of excitation

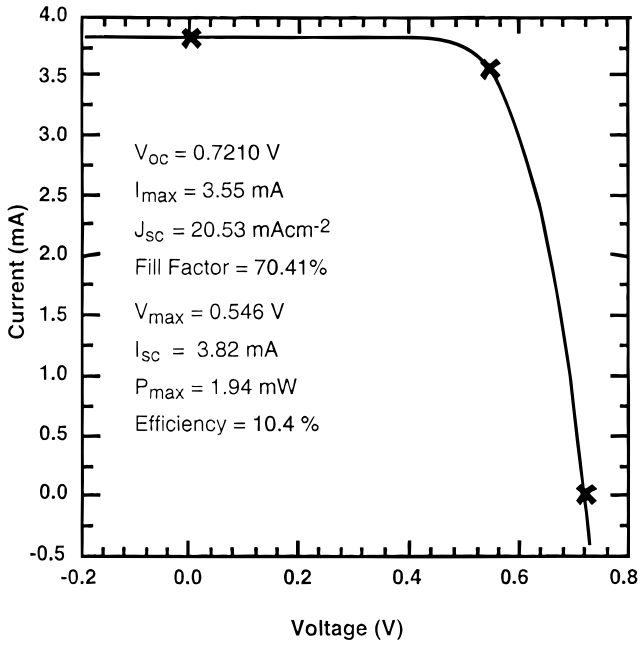

FIGURE 10. Photocurrent−voltage characteristic of a nanocrystalline photoelectrochemical cell sensitized with the panchromatic "black" dye. The results plotted were obained at the NREL calibration laboratory.

wavelength. Both chromophores show very high IPCE values in the visible range. After correction for losses due to light reflection and absorption by the conducting glass, the conversion of photons to electric current is practically quantitative in the plateau region of the curves. However, the response of the black dye extends 100 nm farther into the infrared than that of N3. The photocurrent onset is close to 920 nm, i.e., near the optimal threshold for single junction converters. From there on, the IPCE rises gradually until at 700 nm it reaches a plateau of ca. 80%. If one accounts for reflection and absorption losses in the conducting glass, the conversion of incident photons to electric currents is practically quantitative over the whole visible domain. From the overlap integral of the curves in Figure 9 with the solar emission spectrum, one predicts the short-circuit photocurrents of the N3 and black dye-sensitized cells to be 16.5 and 20.5 mA/cm^2, respectively, in agreement with experimental observations. The overall efficiency (η_{global}) of the photovoltaic cell is calculated from the integral photocurrent density (i_{ph}), the open-circuit photovoltage (V_{oc}), the fill factor of the cell (ff), and the intensity of the incident solar light (I_s = 1000 W/m^2):

$$\eta_{global} = i_{ph} V_{oc} (ff)/I_s$$

At this stage the confirmed efficiency obtained with the black dye is 10.4% under standard air mass 1.5 reporting conditions, as confirmed by the PV calibration laboratory of the National Energy Research Laboratory (NREL, Golden CO). A typical $I-V$ curve is shown in Figure 10. Further development will concentrate on the enhancement of the photoresponse in the near-IR region. Judicious molecular engineering of the black dye structure, e.g., the substitution of the carboxylic acid by *p*-carboxylphenyl groups, will be used to increase the extinction coefficient substantially in the 700−900 nm region. The goal is to obtain a photovoltaic cell having optical features similar to those of GaAs. A nearly vertical rise of the photocurrent close to the 920 nm absorption threshold would increase the short-circuit photocurrent from currently 20.5 to about 28 mA/cm^2. This could raise the overall efficiency to over 15%.

Future Outlook

Mastering the interface is the first challenge for future development of molecular photovoltaics. The high contact area of the junction nanocrystalline solar cells renders mandatory the grasp and molecular control of surface effects for future improvement of cell performance. Synthetic efforts will focus on the design of sensitizers, such as molecular dyads,[48] enhancing the charge separation at the oxide−solution interface. The structural features of the dye should match the requirements for molecular rectification. In analogy to the photofield effect in transistors, the gate for unidirectional electron flow from the redox electrolyte through the junction and into the conduction band of the oxide is opened by the photoexcitation of the sensitizer. The reverse charge flow, i.e., recapture of the electron by the electrolyte, should be impaired by judicious design of the sensitizer: while conducting electrons in the excited state, it should be an insulator in the ground state forming a molecular blocking layer at the heterojunction between the semiconductor and the electrolyte or the solid hole conductor. Molecular gating would benefit greatly the efficiency of the photocell. Even a relatively small increment, of e.g. 200 mV, in the open-circuit voltage would allow the overall solar conversion yield to be raised from currently 10.4 to nearly 15%.

Panchromatic sensitization extending throughout the visible and near-IR regions is another challenge for the future. Dye cocktails have already been applied to mesoporous TiO_2 films in the form of mixtures of porphyrins and phthalocyanines.[48] The result was encouraging inasmuch as the optical effects of the two sensitizers were found to be additive and there was no destructive interference of the dyes. There are many options for dyes that could be combined to improve the photocurrent of the device, opening up a fertile field for further investigations.

An advantage of dye-sensitized solar cells is that they can be used to produce directly high-energy chemicals from sunlight. Such "photosynthetic" devices can overcome the principal problem of all photovoltaic cells, i.e., the lack of capacity for energy storage. The "Holy Grail" of all photoconversion processes is the splitting of water into hydrogen and oxygen by sunlight, and there is no doubt that this will be one of the primary targets of future research.

M.G. expresses his gratitude to co-workers who have contributed to the progress in the research on dye-sensitized solar cells. Support of this work by the Swiss National Science Foundation as well as the Swiss National Energy Office is gratefully acknowledged. Thanks are also due to the industrial licensees of EPFL, in

particular the Institute of Applied Photovoltaics in Gelsenkirchen, Germany, for their collaboration and financial contribution. A.H. thanks the Foundation for strategic environmental research (MISTRA) and the Swedish national energy administration for financial support and the researchers within the consortium of mesoporous systems at Uppsala University for valuable comments and assistance in drawing some of the figures.

References

(1) West, W. Proceedings of the Vogel Centennial Symposium. *Photogr. Sci. Eng.* **1974**, *18*, 35.
(2) Moser, J. Notiz über die Verstärkung photoelektrischer Ströme. *Monatsh. Chem.* **1887**, *8*, 373.
(3) Namba, S.; Hishiki, Y. Color Sensitization of Zinc Oxide with Cyanine Dyes. *J. Phys. Chem.* **1965**, *69*, 774.
(4) Gerischer, H.; Tributsch, H. Elektrochemische Untersuchungen zur Sensibilisierung von ZnO-Einkristallen. *Ber. Bunsen-Ges. Phys. Chem.* **1968**, *72*, 437.
(5) Dare-Edwards, M. P.; Goodenough, J. B.; Hamnet, A.; Seddon K. R.; Wright, R. D. Sensitization of Semiconductor electrodes by Ruthenium-based Dyes. *Faraday Discuss. Chem. Soc.* **1980**, *70*, 285.
(6) Tsubomura, H.; Matsumura, M.; Noyamura, Y.; Amamyiya, T. Dye-sensitized Zinc oxide/aqueous electrolyte/platinum Photocell. *Nature* **1976**, *261*, 402.
(7) Duonghong, D.; Serpone, N.; Grätzel, M. 114. Integrated Systems for Water Cleavage by Visible Light; Sensitization of TiO_2 Particles by Surface Derivatization with Ruthenium Complexes. *Helv. Chim. Acta* **1984**, *67*, 1012−1018.
(8) Desilvestro, J.; Grätzel, M.; Kavan, L.; Moser, J. E.; Augustynski, J. Highly Efficient Sensitization of Titanium Dioxide. *J. Am. Chem. Soc.* **1985**, *107*, 2988−2990.
(9) Vlachopoulos, N.; Liska, P.; Augustynski, J.; Grätzel, M. Very Efficient Visible Light Energy Harvesting and Conversion by Spectral Sensitization of High Surface Area Polycrystalline Titanium Dioxide Films. *J. Am. Chem. Soc.* **1988**, *110*, 1216−1220.
(10) O'Regan, B.; Grätzel, M. A low-cost, high-efficiency solar cell based on dye-sensitized colloidal TiO_2 films. *Nature (London)* **1991**, *335*, 737−739.
(11) Barbe, Ch.; Arendse, F.; Comte, P.; Jirousek, M.; Lenzmann, F.; Shklover, V.; Grätzel, M. Nanocrystalline Titanium Oxide Electrodes for Photovoltaic Applications. *J. Am. Ceram. Soc.* **1997**, *80* (12), 3157−3171.
(12) Tennakone, K.; Kumara, G. R. R. A.; Kumarasinghe, A. R.; Wijayantha, K. G. U.; Sirimanne, P. M. A Dye-sensitized Nanoporous Solid Sate Photovoltaic cell. *Semicond. Sci. Technol.* **1995**, *10*, 1689.
(13) O'Regan, B.; Schwarz, D. T. Efficient Dye-sensitized Charge Separation in a Wide-band-gap p−n Heterojunction. *J. Appl. Phys.* **1996**, *80*, 4749−4754.
(14) Bach, U.; Lupo, D.; Comte, P.; Moser, J. E.; Weissörtel, F.; Salbeck, J.; Spreitzer, H.; Grätzel, M. Solid-state Dye-sensitized Mesoporous TiO_2 Solar Cells with High Photon-to -Electron Conversion Efficiencies. *Nature* **1998**, *395*, 583−585.
(15) Nazeeruddin, M. K.; Kay, A.; Rodicio, I.; Humphry-Baker, R.; Müller, E.; Liska, P.; Vlachopoulos, N.; Grätzel, M. Conversion of Light to Electricity by cis-X_2Bis(2,2′-bipyridyl-4,4′-dicarboxylate)ruthenium-(II) Charge-Transfer Sensitizers (X = Cl^-, Br^-, I^-, CN^-, and SCN^-) on Nanocrystalline TiO_2 Electrodes. *J. Am. Chem. Soc.* **1993**, *115*, 6382−6390.
(16) Amadelli, R.; Argazzi, R.; Bignozzi, C. A,; Scandola, F. Design of Antenna−Sensitizer Polynuclear Complexes. Sensitization of Titanium Dioxide with $[Ru(bpy)_2]_2Ru(bpy(COO)_2)_2$. *J. Am. Chem. Soc.* **1990**, *112*, 7029.
(17) Alebbi, M.; Bignozzi, C. A.; Heimer, T.A.; Hasselmann, G.; Meyer, G. J. The limiting Role of Iodide Oxidation in cis-$Os(dcb)_2(CN)_2$/TiO_2 Photoelectrochemical Cells *J. Phys. Chem. B* **1998**, *102*, 7577.
(18) Nazeeruddin, Md. K.; Péchy, P.; Grätzel, M. Efficient panchromatic sensitization of nanocrystalline TiO_2 films by a black dye based on a trithiocyanato-ruthenium complex. *Chem. Commun.* **1997**, 1705−1706.
(19) Kohle, O.; Ruile, S.; Grätzel, M. Ruthenium(II) Charge-Transfer Sensitizers Containing 4,4′-Dicarboxy-2,2′-bipyridine. Synthesis, Properties, and Bonding Mode of Coordinated Thio- and Selenocyanates. *Inorg. Chem.* **1996**, *35*, 4779−4787.
(20) Shklover, V.; Ovchinnikov, Yu E.; Braginsky, L. S.; Zakeeruddin, S. M.; Grätzel, M. Structure of Organic/Inorganic Interface in Assembled Materials Comprising Molecular Components. Crystal Structure of the Sensitizer Bis[4,4′-carboxy-2,2′-bipyridine)(thiocyanato)]ruthenium(II). *Chem. Mater.* **1998**, *10*, 2533−2541.
(21) Finnie, K. S.; Bartlett, J. R.; Woolfrey, J. L. Vibrational Spectroscopic Study of the Coordination of (2,2′-Bipyridyl-4,4′-dicarboxylic acid)ruthenium (II) Complexes to the Surface of Nanocrystalline Titania. *Langmuir* **1998**, *14*, 2744.
(22) Patthey, L.; Rensmo, H.; Persson, P.; Westermark, K.; Vayssieres, L.; Stashans, A.; Petersson, P.; Brohwiler, P. A.; Siegbahn, H.; Lunell, S.; Martensson, N.; Adsorption of bi-isonicotinic acid on rutile TiO_2 (110). *J. Chem. Phys.* **1999**, *110*, 5913.
(23) Rensmo, H.; Lunell, S.; Siegbahn, H. Absorption and electrochemical properties of ruthenium(II) dyes, studied by semi-empirical quantum chemical calculations. *J. Photochem. Photobiol. A* **1998**, *114*, 117−124.
(24) Rensmo, H.; Södergren, S.; Patthey, L.; Westermark, K.; Vayssieres, L.; Kohle, O.; Brohwiler, P. A.; Hagfeldt, A.; Siegbahn, H. The electronic structure of the cis-bis(4,4′-dicarboxy-2,2′-bipyridine)-bis(isothiocyanato)ruthenium(II) complex and its ligand 2,2′-bipyridyl-4,4′-dicarboxylic acid studied with electron spectroscopy. *Chem. Phys. Lett.* **1997**, *274*, 51−57.
(25) Hagfeldt, A.; Grätzel, M. Light-Induced Redox Reactions in Nanocrystalline Systems. *Chem. Rev.* **1995**, *95*, 49−68.
(26) Tachibana, Y.; Moser, J. E.; Grätzel, M.; Klug, D. R.; Durrant, J. R. Subpicosecond Interfacial Charge Separation in Dye-Sensitized Nanocrystalline Titanium Dioxide Films. *J. Phys. Chem.* **1996**, *100*, 20056−20062.
(27) Hannappel, T.; Burfeindt, B.; Storck, W.; Willig, F. Measurement of Ultrafast Photoinduced Electron Transfer from Chemically Anchored Ru−Dye Molecules into Empty Electronic States in a Colloidal Anatase TiO_2 Film. *J. Phys. Chem. B* **1997**, *101*, 6799−6802.
(28) Moser, J. E.; Noukakis, D.; Bach, U.; Tachibana, Y.; Klug, D. R.; Durrant, J. R.; Humphry-Baker, R.; Grätzel, M. Comment on "Measurement of Ultrafast Photoinduced Electron Transfer". *J. Phys. Chem. B* **1998**, *102*, 3649−3650.
(29) Das, S.; Kamat, P. V. Spectral Characterization of the One-Electron Oxidation Product of cis-Bis(isothiocyanato)bis(4,4′-dicarboxylato-2,2′-bipyridyl) Ruthenium(II) Complex Using Pulse Radiolysis. *J. Phys. Chem. A* **1998**, 102, 8954.
(30) Ashbury, J. B.; Ellingson, R. J.; Ghosh, H. N.; Ferrere, S.; Nozik, A. J.; Lian, T. Femtosecond IR Study of Excited-State Relaxation and Electron-Injection, Dynamics of $Ru(dcbpy)_2(NCS)_2$ in Solution and on Nanocrystalline TiO_2 and Al_2O_3 Thin Films. *J. Phys. Chem. B* **1999**, *103*, 3110−3119.
(31) Heimer, T. A.; D'Arcangelis, S. T.; Farzad, F.; Stipkala, J. M.; Meyer, G. Enhanced Spectral Sensitivity from Ru(II)Polypyridyl Photovoltaic Devices. *Inorg. Chem.* **1996**, *35*, 5319.
(32) Ferrere, S.; Gregg, B. A. Photosensitization of TiO_2 by [FeII(2,2′-bipyridine-4,4′-dicarboxylic acid)$_2$$(CN)_2$]: Band Selective Electron Injection from Ultra-Short-Lived Excited States. *J. Am Chem. Soc.* **1998**, *120*, 843.
(33) Moser, J. E.; Grätzel, M. Excitation-Wavelength Dependence of Photoinduced Charge Injection at the Semiconductor-Dye Interface: Evidence for Electron Transfer from Vibrationally Hot Excited States. *Chimia* **1998**, *52*, 160−162.
(34) Moser, J. E.; Grätzel, M. Observation of temperature independent heterogeneous electron-transfer reactions in the inverted Marcus region. *Chem. Phys.* **1993**, *176*, 493−500.
(35) Haque, S. A.; Tachibana, Y.; Klug, D. R.; Durrant, J. R. Charge recombination kinetics in dye-sensitized nanocrystalline titanium dioxide films under externally applied bias. *J. Phys. Chem. B* **1998**, *102*, 1745−1749.
(36) Ferber, J.; Stangl, R.; Luther, J. An Elecrical Model for Dye-sensitzed Solar Cells. *Sol. Energ. Mater. Solar. Cells* **1998**, *53*, 29.
(37) Schlichthörl, G.; Huang, S. Y.; Sprague, J.; Frank, A. J. Band edge movement and recombination kinetics in dye-sensitized nanocrystalline TiO_2 solar cells: A study by intensity modulated photovoltage spectroscopy. *J. Phys. Chem. B* **1997**, *101*, 8141−8155.
(38) Bond, A. M.; Deacon, G. B.; Howitt, J.; Mac Farlane, D. R.; Spiccia, L.; Wolfbauer, G. Voltammetric determination of the Reversible Redox Potential for the oxidation of the Highly Surface Active Polypyridyl Ruthenium Photovoltaic Sensitizer *cis*-Ru(II)$(dcbpy)_2$-$(NCS)_2$. *J. Electrochem. Soc.* **1999**, *146*, 648.
(39) Södergren, S.; Hagfeldt, A.; Olsson, J.; Lindquist, S.-E. Theoretical models for the action spectrum and the current−voltage characteristics of microporous semiconductor films in photoelectrochemical cells. *J. Phys. Chem.* **1994**, *98*, 5552−5556.
(40) Cao, F.; Oskam, G.; Meyer, G. J.; Searson, P. S. Electron Transport in Porous Nanocrystalline TiO_2 Photoelectrotrchemical Cells. *J. Phys Chem.* **1996**, 100, 17021−17027.
(41) Dloczik, L.; Ileperuma, O.; Lauermann, I.; Peter, L. M.; Ponomarev, E. A.; Redmond, G.; Shaw, N. J.; Uhlendorf, I.; Dynamic Response of Dye-sensitized Nanocrystalline Solar Cells: Characterisation by Intensity-Modualted Photocurrent Spectroscopy. *J. Phys. Chem. B* **1997**, *101*, 10281.

(42) Vanmaekelbergh, D.; de Jongh, P. E. Driving Force for Electron Transport in Porous Nanostructured Photoelectrodes. *J. Phys. Chem. B* **1999**, *103*, 747−750.
(43) Nelson, J. Continuous-time random-walk model of electron transport in nanocrystalline TiO_2 electrodes. *Phys. Rev. B* **1999**, *59*, 15374−15380.
(44) Scher, H.; Montroll, E. W. Anomalous transit-time dispersion in amorphous solids. *Phys. Rev. B* **1975**, *12*, 2455.
(45) Solbrand, A.; Södergren, S.; Lindström, H.; Rensmo, H.; Hagfeldt, A.; Lindquist, S.-L. Electron transport in the nanostructured TiO_2-electrolyte system studied with time-resolved photocurrents. *J. Phys. Chem. B* **1997**, *101*, 2514−2518.
(46) Papageorgiou, N.; Grätzel, M.; Infelta, P. P. On the Relevance of Mass Transport in thin Layer Nanocrystalline Photoelectrochemical Solar Cells. *Sol. Energy Mater. Sol. Cells* **1996**, *44*, 405−438.
(47) Wahl, A.; Augustynski, J. Charge carrier transport in nanostructured anatase TiO_2 films assisted by the self-doping of nanoparticles. *J. Phys. Chem. B* **1998**, 7820−7828.
(48) Argazzi, R.; Bignozzi, C. A.; Heimer, T. A.; Castellano, F. N.; Meyer; G. J. Light-Induced Charge Separation across Ru(II)-Modified Nanocrystalline TiO_2 Interfaces with Phenothiazine Donors. *J. Phys. Chem.* **1997**, *101*, 2591−2597.
(49) Fang, J.; Su, L.; Wu, J.; Shen, Y.; Lu, Z. Fabrication, Characterization an Photovoltaic Studies of Dye Co-modified TiO_2 Electrodes. *New J. Chem.* **1997**, *270*, 145.

AR980112J